

Figure S1. Simulated annual-mean rainfall in MOD experiment (A) compared to CRU dataset (B). Figure (C) represent the seasonal cycles of precipitation spatially averaged from 25°N to 40°N and from 75°E to 100°E for the MOD experiment (green) and for the CRU dataset (orange).

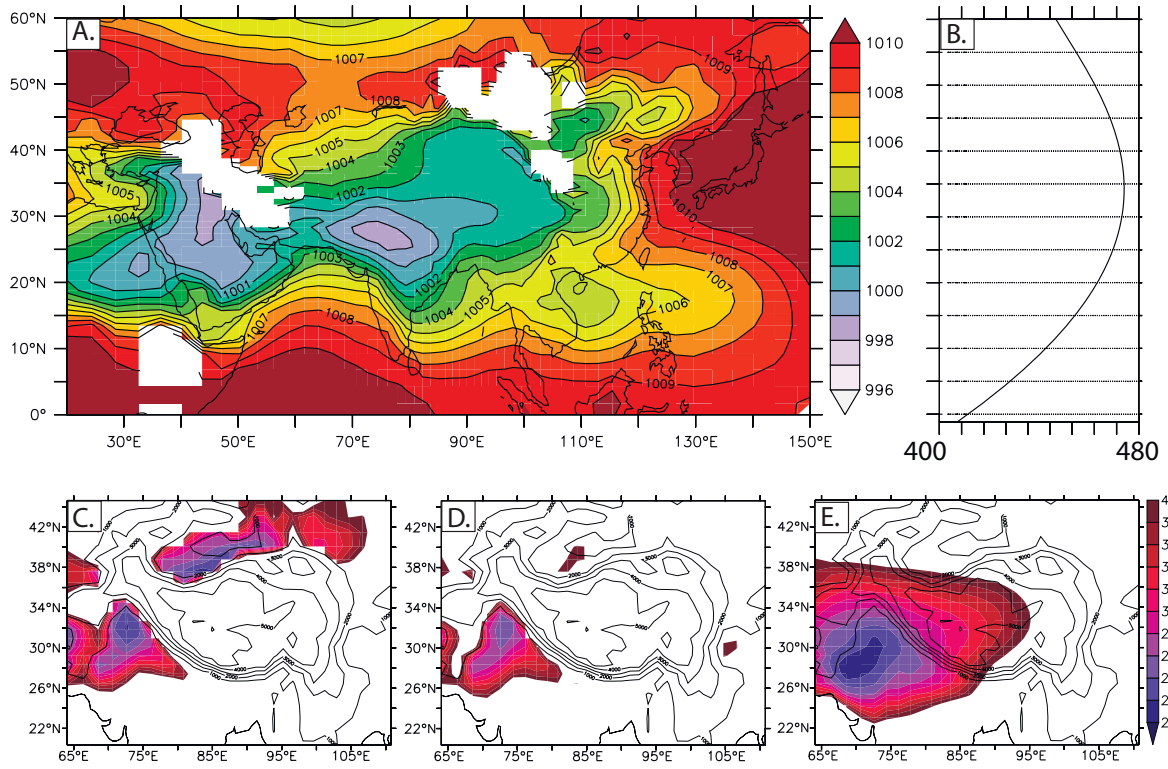


Figure S2. (A) Mean annual sea level pressure (hPa) for the LOW simulation, (B) Meridional transect of the insolation at the top of atmosphere ( $\text{W m}^{-2}$ ), averaged for  $90^\circ\text{E}$ , (C, D, E) Regions where relative humidity is under 40% for (C) MOD, (D) INT and (E) LOW experiment.

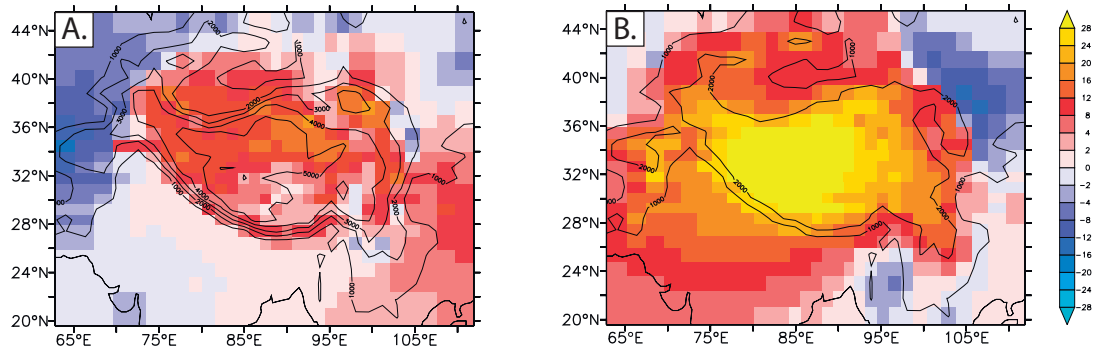


Figure S3. Total cloudiness change for A) MOD-INT B) INT-LOW cases.

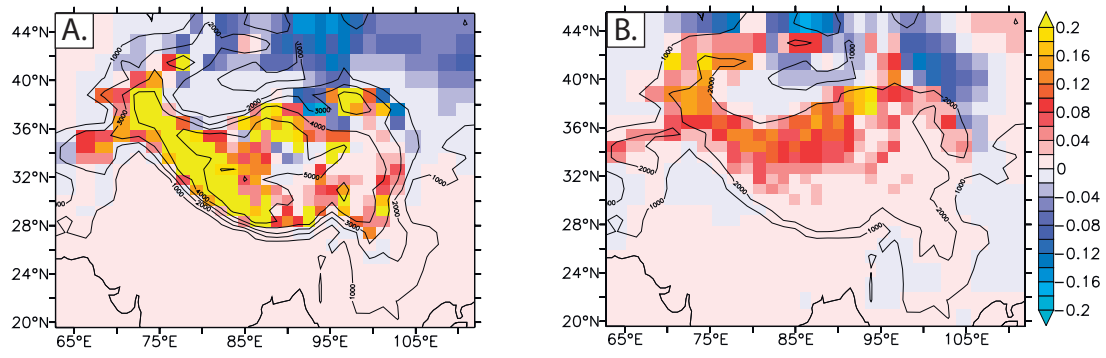


Figure S4. Surface albedo change for (A) MOD-INT (B) INT-LOW cases

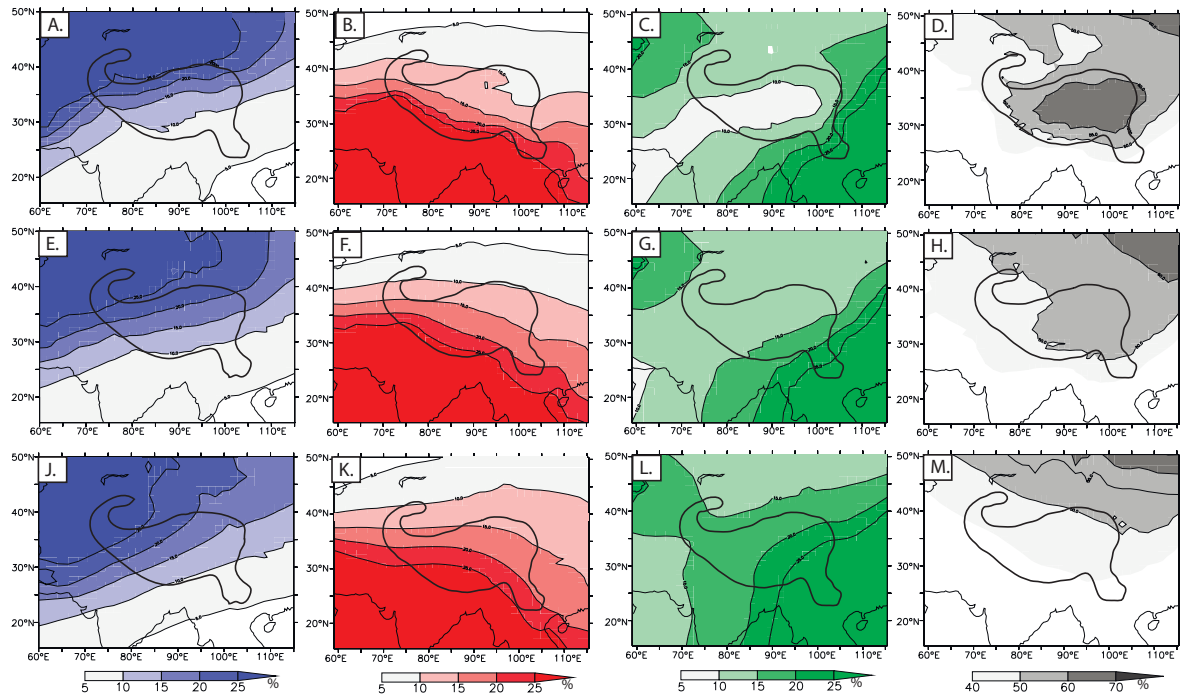


Figure S5. Moisture sources changes, illustrated by vertically integrated portion of vapour having evaporated over different regions. Blue shade - the Atlantic Ocean and Mediterranean sea source, red - the Indian Ocean moisture source, green - the Pacific Ocean source, grey - continental recycling source . (A, B, C, D) - MOD case, (E, F, G, H) - INT case, (J, K, L, M) - LOW case.

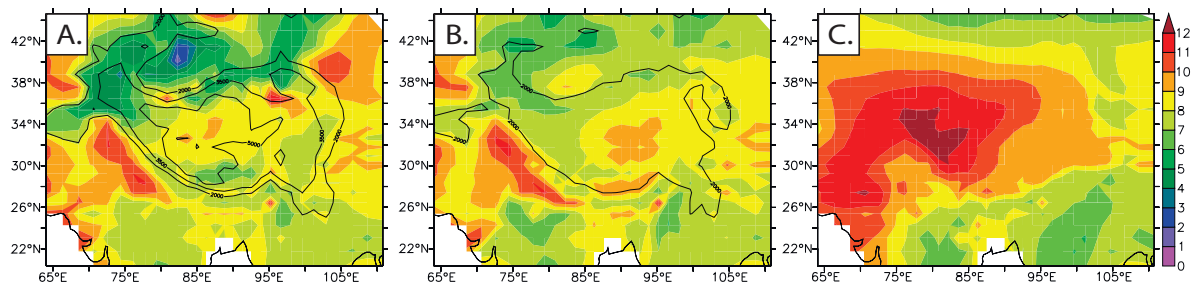


Figure S6. Deviations of precipitation  $\delta^{18}\text{O}$  from the vapour composition,  $\epsilon = R_p - R_v$  for (A) MOD, (B) INT and (C) LOW cases